공학석사학위논문

회분식 고분자 세척공정의 기초적 모델링 및 실험적 연구

Fundamental Modeling and Experimental Investigation of Polymer Washing Batch Process

2016년 2월

서울대학교 대학원
화학생물공학부
손 상 환

Abstract

After polymerization reaction, impurities composed of adduct, used solvent and catalyst remain inside the formed polymers. These impurities should be removed by washing to improve the purity of the polymers. In this process, the model of the polymer washing process is essential to optimize the energy, resources and operating time. This work proposes a fundamental model of polymer washing process to provide theoretical basis for optimization. The model describes the impurity distribution inside the polymers using pseudo steady state approximation with the concept of moving boundary of diffusion. Also, the impurity diffusion at polymer surface is described with Fick′s law.

In addition, this work reports an experimental investigation of polymer washing process using SPAEK (sulfonated poly(aryl ether ketone)) samples. In the investigation, impurity diffusion coefficient at polymer surface of the experiment is computed from the pH data. The computed D have different values for each operation, as a lumped parameter. However these values show the same trajectory with the introduction of a dimensionless number Co for each operation. This means other impurity diffusion factors, not included in the model, embraced in D are only affected by Co, even if the initial impurity concentrations inside the polymers are different for each operation.

Finally, we predict the pH changes in a different experimental condi-

tion, and validate the prediction performance of the model.

Keyward : Polymer washing process, Moving boundary of diffusion, Pseudo steady state, Sulfonated poly(aryl ether ketone)

Student number : 2014-20583

Contents

List of Figures

List of Tables

Chapter 1

Introduction

A polymerization is a chemical reaction in which monomers molecules combine together to form a larger polymer. Polymerization is commonly used in synthesis of industrial macromolecules such as poly(lactic acid), hyperbranched polyamides and poly(2-alkoxypyridine-3,5-diyl)[1, 2, 3]. Especially, SPAEK and sulfonated polyimides used for proton exchange membrane in fuel cell are synthesized by condensation polymerization[4, 5]. In polymerization reaction, aprotic polar solvents such as NMP (N-Methyl-2-pyrrolidone) and DMSO (Dimethyl sulfoxide) are commonly used as solvent and metal carbonates containing alkali metals such as Na and K are used as catalyst. On the completion of reaction, the produced polymer is solidified in other solvent. In this process, a small amount of adduct, solvent and catalyst components are still trapped inside the polymers in the solidification process. Therefore, a washing process is necessary to remove these impurities and improve the purity of polymers, which has a significant influence on microstructural characteristic of polymer product such as polymer membranes. [6, 7].

However theoretical research about polymer washing process after polymerization reaction has not been reported yet to the best of the authors' knowledge. It is just only described in some papers dealing with the synthe-

sis process of polymer, as solidified polymers being washed repeatedly with deionized water until the pH of washing water reaching 6-7 at a lab scale [4, 8]. When polymer washing process is operated at a large scale without any optimization of operating conditions such as amount of washing water, number of operations and operating time for each operations, the waste of energy, resources and time will be considerable. Moreover, such a complex dynamics involving mass transfer in the polymer particulate is difficult to model using an empirical model structure fitted to operational data. This work presents a fundamental mathematical model and an experimental investigation of a polymer washing batch process which can be readily used for optimization of the process.

In polymer washing process, the solidified polymers are washed by deionized water in batch several times with stirring. Before washing process begins, impurity concentrations inside the polymers are maintained as the initial concentration. When washing begins, the impurities inside the polymers are dissolved in washing water and diffuse toward outside with the concentration gradient. As the washing process proceeds, the impurity concentration of the polymer inside decreases and that in batch increases. When impurity concentrations of the polymer inside and batch inside reach the equilibrium, the impurity concentrations stop changing. These processes are repeated until the pH in batch reaching near 7.

This work introduces the concept of moving boundary of diffusion inside the polymers, where impurities begin to diffuse toward outside, to model the impurity diffusion inside the polymers [9, 10]. The model employs Pseudo steady state approximation for impurity distribution inside the

polymers, represents impurity diffusion rate with Fick′s law, and includes mole balance of impurities. In addition, we estimate the mathematical relationship between pH and impurity concentration in batch and D values using the experimental data of SPAEK sample. Since we develop the model with Fick′s law, the computed D has time varying values as a lumped parameter embracing other factors of impurity diffusion. A dimensionless number Co, the ratio of impurity concentration in batch to initial impurity concentration inside the polymers, is introduced to model temporal change of the diffusion coefficient regardless of the initial concentration of the impurity inside the polymers. Then, we numerically simulate the radius changes of diffusion boundary for the experiments using the estimated D and analyze the result. Finally, we predict the pH changes in a different experimental condition and compare them with the experimental data. The predicted results are in agreement with the experimental results, and the proposed model and experimental investigation methodology are expected to be useful for optimization of the polymer washing process.

Chapter 2

Modeling

A conceptual model of polymer washing process is constructed as follows. The impurity distributions inside the polymers are uniform as the initial concentration prior to washing, then the distributions change with impurity diffusion toward outside due to the concentration gradient as the washing progress. Finally the impurity distribution stops changing at the equilibrium state where the impurity concentrations of polymer inside and batch inside are equal. After the operation, the used water is removed from the batch and a new batch of operation starts with fresh water. The initial impurity distributions inside the polymers are considered to be the same as the final distributions of the previous operation.

This work develops the model describing the impurity distribution change inside the polymer using the following assumptions. The shapes of the polymers are sphere, radii of the polymers are same, impurities are uniformly distributed inside the polymers except radial direction, impurities diffuse by only molecular diffusion according to concentration gradient, impurity concentration gradient and diffusion inside the polymers occur only in radial direction, the amounts of water inside the polymers are same, impurity distribution changes inside the polymers are identical for all polymers, and impurity concentration in batch changes uniformly regardless of location

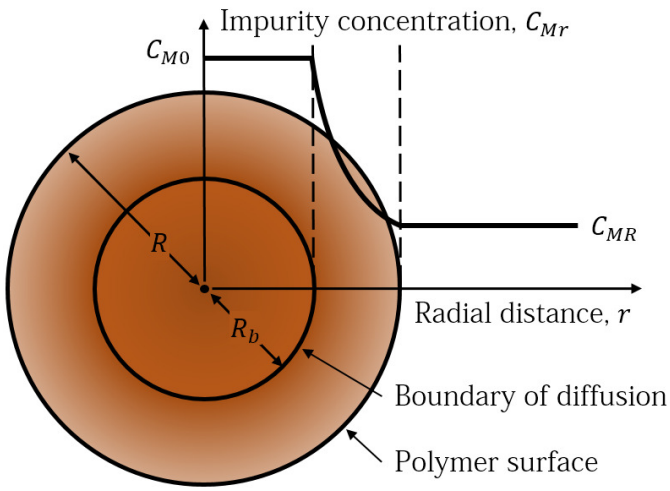

Figure 1: Distribution of the impurity concentration inside the polymer.

due to stirring.

We define the moving boundary of diffusion as the boundary where the impurities start diffusing along the concentration gradient toward outside, and the impurity concentration inside the diffusion boundary remains as the initial concentration (see Fig. 1). R and R_b are the radii of the polymer and of the diffusion boundary, respectively. R_b decreases with the progress of washing process (see Fig. 2). When the diffusion boundary reaches the center of the polymer, impurity concentrations of polymer inside and batch inside are in equilibrium state.

2.1 Pseudo steady state approximation of impurity distribution inside the polymer

As the washing process proceeds, the impurities diffuse in radial direction from the diffusion boundary. The radius of diffusion boundary is the same as the polymer radius prior to washing, and then decreases toward the center with the progress of washing. This is an unsteady state process where the distribution of impurities and the radius of diffusion boundary change with time. Since we assume the impurity diffusion occurs only by molecular diffusion according to the concentration gradient and most of materials have small values of molecular diffusion coefficients in water near $10^{-5} cm^2/s$ [11], we use pseudo steady state approximation to describe the distribution of impurities inside the polymer [12, 13]. We consider the differential volume inside the polymer illustrated in Fig. 2. The pseudo steady state equation of impurities is described as

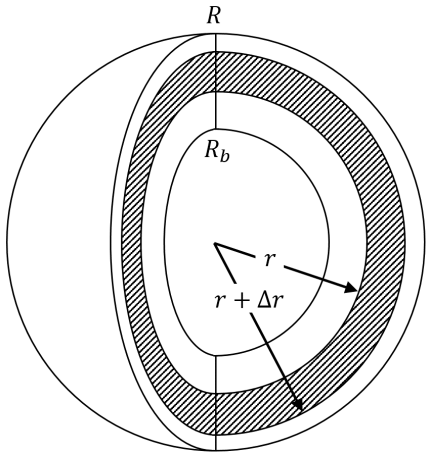

Figure 2: Differential volume inside the polymer.

$$W_{Mr}4\pi r^2|_r - W_{Mr}4\pi r^2|_{r+\Delta r} = 0 \tag{2.1}$$

W_{Mr} is the radial flux of impurities and M means the impurities. Since we assume the impurity diffusion occurs only by molecular diffusion, W_{Mr} is described by the Fick′s law :

$$W_{Mr} = -D_p \frac{dC_{Mr}}{dr} \tag{2.2}$$

where C_{Mr} is the impurity concentration according to radial distance from the polymer center and D_p is the impurity diffusion coefficient inside the polymer. Substituting Eq. (2.2) into Eq. (2.1) and integrating yields

$$C_{Mr} = \frac{-K_1}{r} + K_2 \tag{2.3}$$

where K_1 and K_2 are the integration constants. Boundary conditions are

$$C_{Mr} = C_{MR} \quad at \quad r = R \tag{2.4}$$

$$C_{Mr} = C_{M0} \quad at \quad r = R_b \tag{2.5}$$

C_{MR} is the impurity concentration at the polymer surface and has the same value of the impurity concentration in batch. C_{M0} is the impurity concentration inside the diffusion boundary and same as the initial concentration.

Substituting Eq. (2.4) and Eq. (2.5) into Eq. (2.3) yields,

$$C_{Mr} = \frac{(C_{M0} - C_{MR})\frac{1}{r} + C_{MR}\frac{1}{R_b} - C_{M0}\frac{1}{R}}{\frac{1}{R_b} - \frac{1}{R}} \tag{2.6}$$

Eq. (2.6) represents the impurity concentration profile inside the polymers from diffusion boundary to polymer surface.

2.2 Mole balance of impurities inside the polymer and in batch

We set up a mole balance equation of impurities inside the polymer and in batch to derive a mathematical relationship between diffusion boundary radius and impurity concentration in batch which we can estimate from the pH data. Since the initial amount of impurities in batch is zero, the amount of impurities in batch is the same as the change in the amount of impurities inside the polymers :

$$M_{out} = \left(\frac{4}{3}\pi R^3 C_{M0} - \int_0^{R_b} 4\pi r^2 C_{M0} dr - \int_{R_b}^{R} 4\pi r^2 C_{Mr} dr\right) n\phi \tag{2.7}$$

where M_{out} is the amount of impurities in batch, ϕ is the ratio of water volume inside the polymers to volume of polymers, and n is the number of polymer pieces in batch. Substituting Eq. (2.6) into Eq. (2.7) and expressing M_{out} as the product of the water amount and impurity concentration in batch

yields :

$$VC_{MR} = \frac{2}{3}\pi(C_{M0} - C_{MR})(2R^3 - RR_b^2 - R^2R_b)n\phi \tag{2.8}$$

where V is the amount of water in batch. Rearranging Eq. (2.8) by R and C_{MR_b} results in Eq. (2.9) and Eq. (2.10), respectively :

$$R_b = \frac{-R + \sqrt{9R^2 - \frac{6V}{\pi n\phi R}(\frac{C_{MR}}{C_{M0} - C_{MR}})}}{2} = \frac{-R + f(C_{MR})}{2} \tag{2.9}$$

$$C_{MR} = \frac{2\pi n\phi(2R^3 - RR_b^2 - R^2R_b)C_{M0}}{3V_{out} + 2\pi n\phi(2R^3 - RR_b^2 - R^2R_b)} = \frac{g(R_b)}{3V + g(R_b)}C_{M0} \tag{2.10}$$

2.3 Impurity diffusion rate at polymer surface

Diffusion rate of impurities at polymer surface is expressed as the product of the surface area and the radial flux described by the Fick′s law. The diffusion rate is the same as the increasing rate of the impurity amount in batch :

$$4\pi nR^2D\left(-\frac{dC_{Mr}}{dr}|_{r=R}\right) = V\frac{dC_{MR}}{dt} \tag{2.11}$$

Substituting Eq. (2.6) into Eq. (2.11) yields

$$4\pi nD\left(\frac{C_{M0} - C_{MR}}{\frac{1}{R_b} - \frac{1}{R}}\right) = V\frac{dC_{MR}}{dt} \tag{2.12}$$

Substituting Eq. (2.9) into Eq. (2.12) and rearranging yield

$$D = \frac{V_{out}}{4\pi nR(C_{M0} - C_{MR})} \left\{ \frac{3R - f(C_{MR})}{-R + f(C_{MR})} \right\} \frac{dC_{MR}}{dt} \tag{2.13}$$

D is the diffusion coefficient of impurity at polymer surface, which embraces other impurity diffusion factors not included in the model as a lumped parameter. Diffusion coefficient is commonly used as a lumped parameter to establish dynamic models with intrinsic mechanistic relations [14, 15].

Chapter 3

Experimental Investigation

We performed polymer washing experiments with SPAEK samples synthesized by condensation reaction and solidified in ethanol. Since DMSO (dimethyl sulfoxide) and K_2CO_3 (potassium carbonate) are used as the solvent and the catalyst respectively, and KF (potassium fluoride) is the adduct in SPAEK condensation reaction, these materials are considered as the components of the impurities trapped inside the polymers. We washed 3g of the polymer samples with 40ml of 50°C deionized water for 30 minutes in each operation. The experimental condition is described in Table 1. Since the most impurity components were K_2CO_3 and there exist little amount of KF and DMSO, we consider the impurities as K_2CO_3 and the dissociation constant of impurity is considered as the dissociation constant of K_2CO_3.

The 8 batch runs of washing were performed for each two experiments,

Table 1: Summary of the experimental condition.

Condition	Value	Unit
Average radius of polymers, R	0.7	cm
Volume of polymers, V_p	7	ml
Volume of water in batch, V	40	ml
Volume of water inside the polymers, V_{in}	4.2	ml
Volume ratio of polymer inner water to polymers, ϕ	0.60	
Number of polymer pieces, n	5	
Mass of polymers, m	3	g

and the pH in batch was measured at intervals of 10 seconds. The experimental data is illustrated in Fig. 3. The red line is the 1st operation data and the blue lines are the 2-8th operation data. The data of each operation show a certain trend except that of the 1st operation. pH rapidly increases in the beginning, then pH increasing rate gradually becomes slower. Finally pH stops increasing and reaches the equilibrium state. Only the 1st operation data shows the decreasing trend. This difference is mainly attributed to the physical properties of impurity components. KF and K_2CO_3 dissociate into ions in water as weak bases [16, 17]. Though DMSO has an acidity when it dissociates into ions, it hardly ionizes in water and usually does not affect the pH [18]. In the case of the experiments, we speculate that the high basicity due to the high concentration of K_2CO_3 in the 1st operation triggers the DMSO dissociation and pH decreases by the acidity of dissociated DMSO.

Using the experimental data, we derive the relationship between $[OH^-]$ (hydroxide ion concentration) and C_{MR}, compute D values for each operation using the relation, obtain a consistent trajectory of D values using the dimensionless number Co, and numerically simulate the radius change of diffusion boundary inside the polymers.

3.1 Relationship between hydroxide ion concentration and impurity concentration

With the experimental data, we derive the relation between $[OH^-]$ and C_{MR} from those values at equilibrium for each operation (see Table 2). The $[OH^-]$ and C_{MR} values at equilibrium are computed using the ionization

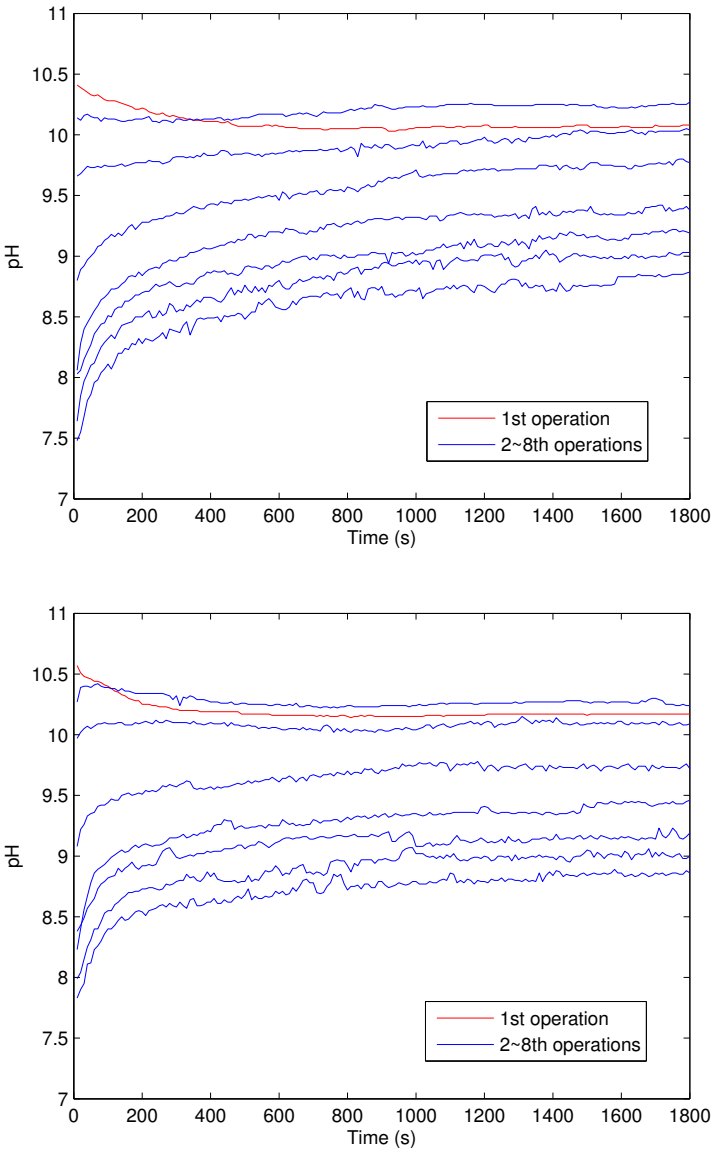

Figure 3: pH data of (a) Experiment 1 (b) Experiment 2.

constant of $50^{\circ}C$ water and dissociation constant of K_2CO_3 with the relationship between the impurity concentration at equilibrium of the nth operation and that of the n-1th operation, respectively. Since the amounts of wash water in batch for each operation were the same, the relationship is described as

$$C_{ME,n} = \frac{V_{in}}{V + V_{in}} C_{ME,n-1} \tag{3.1}$$

where $C_{ME,n}$ and $C_{ME,n-1}$ are the impurity concentrations at equilibrium of the nth and that of the n-1th operation, respectively, V_{in} and V are the amounts of water inside the polymer and in batch, respectively.

The relation between $[OH^-]$ and C_{MR} is estimated by a straight line approximation in log scale using the values in Table 2 as shown in Fig. 4 and Eq. (3.2).

$$C_{MR} = 10^{9.41}[OH^-]^{4.03} \tag{3.2}$$

Table 2: Calculated $[OH_E^-]_n$ and $C_{ME,n}$ values of performed experiments.

Batch	$[OH_E^-]_n$		$C_{ME,n}$	
(n)	Experiment 1	Experiment 2	Experiment 1	Experiment 2
1	2.10e-03	2.50e-03	2.70e-02	3.77e-02
2	9.77e-04	1.00e-03	2.56e-03	3.57e-03
3	5.89e-04	6.76e-04	2.43e-04	3.39e-04
4	3.22e-04	3.24e-04	2.30e-05	3.21e-05
5	1.50e-04	1.55e-04	2.18e-06	3.04e-06
6	8.70e-05	8.94e-05	2.07e-07	2.89e-07
7	6.30e-05	6.37e-05	1.96e-08	2.74e-08
8	3.97e-05	4.27e-05	1.86e-09	2.59e-09

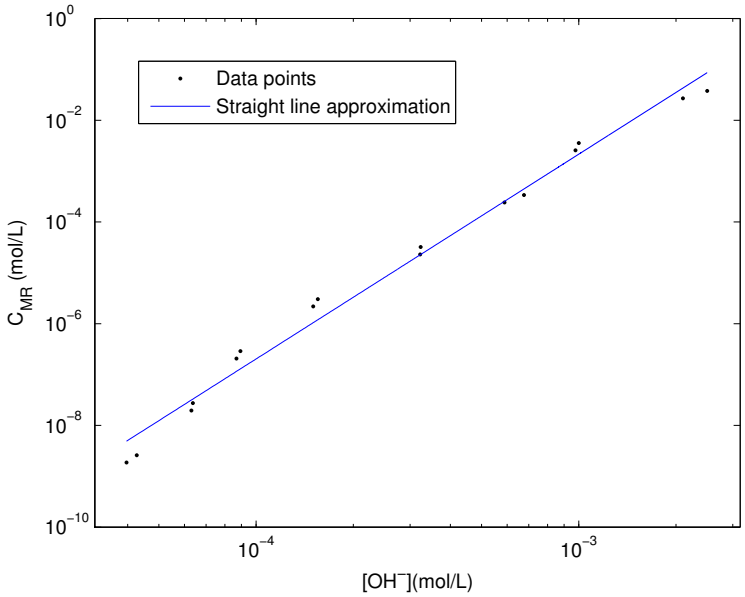

Figure 4: Straight line approximation of impurity concentration according to hydroxide ion concentration.

3.2 Impurity diffusion coefficient at polymer surface

We compute C_{MR} values with time of each operation using Eq. (3.2) and the pH data as shown in Fig. 5. We use the data of the 4-8$^{\text{th}}$ operations showing the regular trend without the influence of DMSO dissociation. Then, we compute D as a function of time in each operation by substituting the obtained C_{MR} values and the experimental condition in Table 1 into Eq. (2.13). The computed D values of each operation are illustrated in Fig. 6.

Whereas the computed D values show quite large differences in time

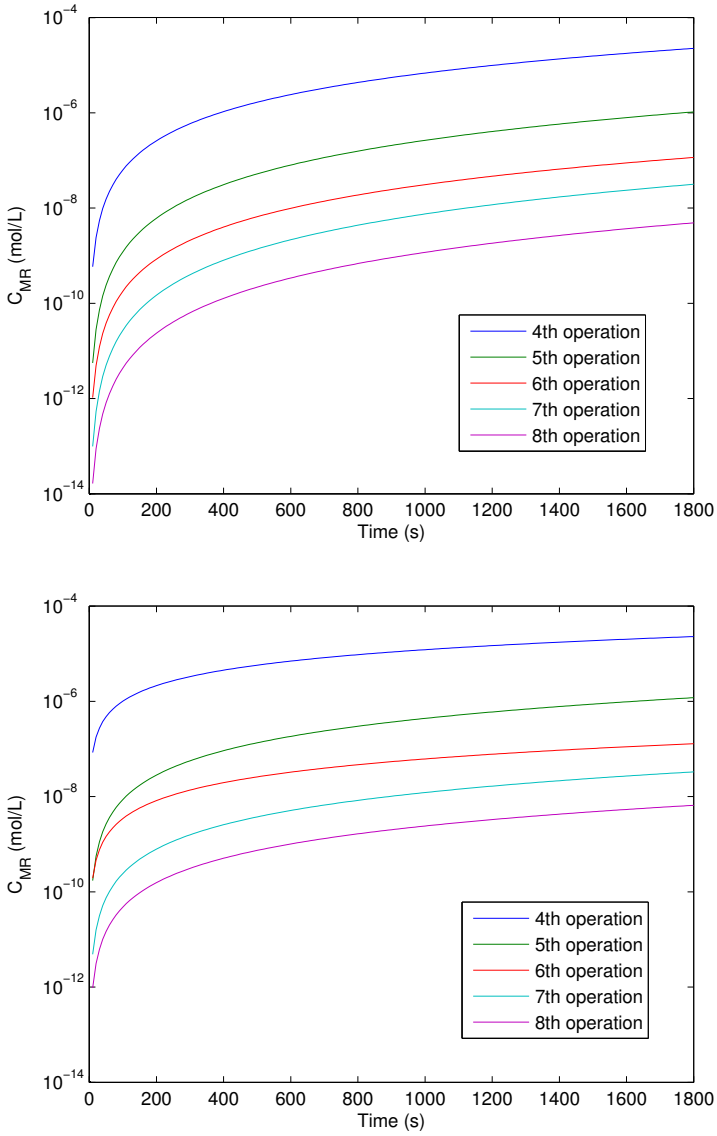

Figure 5: Computed impurity concentration in batch of the 4-8th operations (a) Experiment 1 (b) Experiment 2.

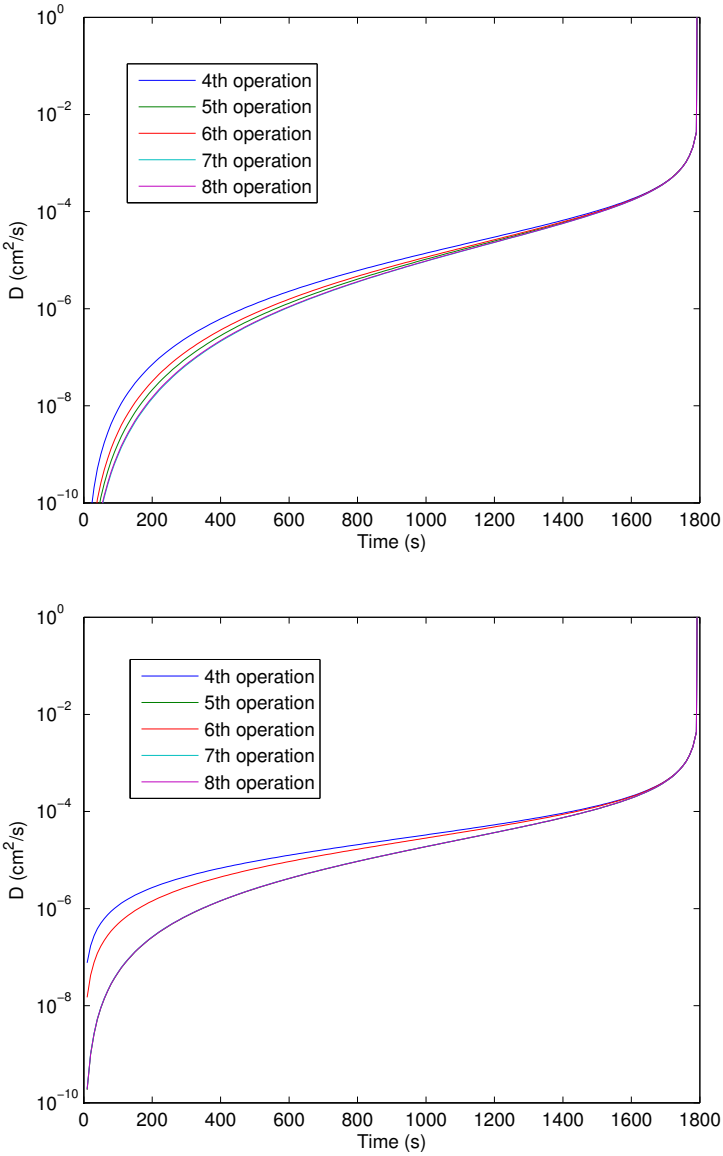

Figure 6: Computed impurity diffusion coefficient of the 4-8th operations (a) Experiment 1 (b) Experiment 2.

as a lumped parameter, D values of each operation show the similar values with a certain temporal trend. This means the impurity diffusion at polymer surface of each operation occur in a similar manner, though the computed C_{MR} shows quite different values for each operation. Thus, we hypothesize this similar aspect is related to the ratio of C_{MR} to C_{M0} and introduce the following dimensionless number :

$$Co = \frac{C_{MR}}{C_{M0}} \tag{3.3}$$

Describing Eq. (2.13) with Co results in

$$D = \frac{V}{4\pi nR(1-Co)}\left(\frac{3R-F(Co)}{-R+F(Co)}\right)\frac{dCo}{dt}, \quad F(Co) = \sqrt{9R^2 - \frac{6V}{\pi n\phi R}\left(\frac{Co}{1-Co}\right)} \tag{3.4}$$

Fig. 7 shows the D values computed from Eq. (3.4). The computed D values according to Co of each operation show almost the same trajectory. This means other impurity diffusion factors embraced in D are only affected by Co, even if the initial impurity concentrations inside the polymers are different for each operation. We approximated the relationship between D and Co as a straight line in log scale. D is described as

$$D = 10^{-2.25}Co^{1.67} \tag{3.5}$$

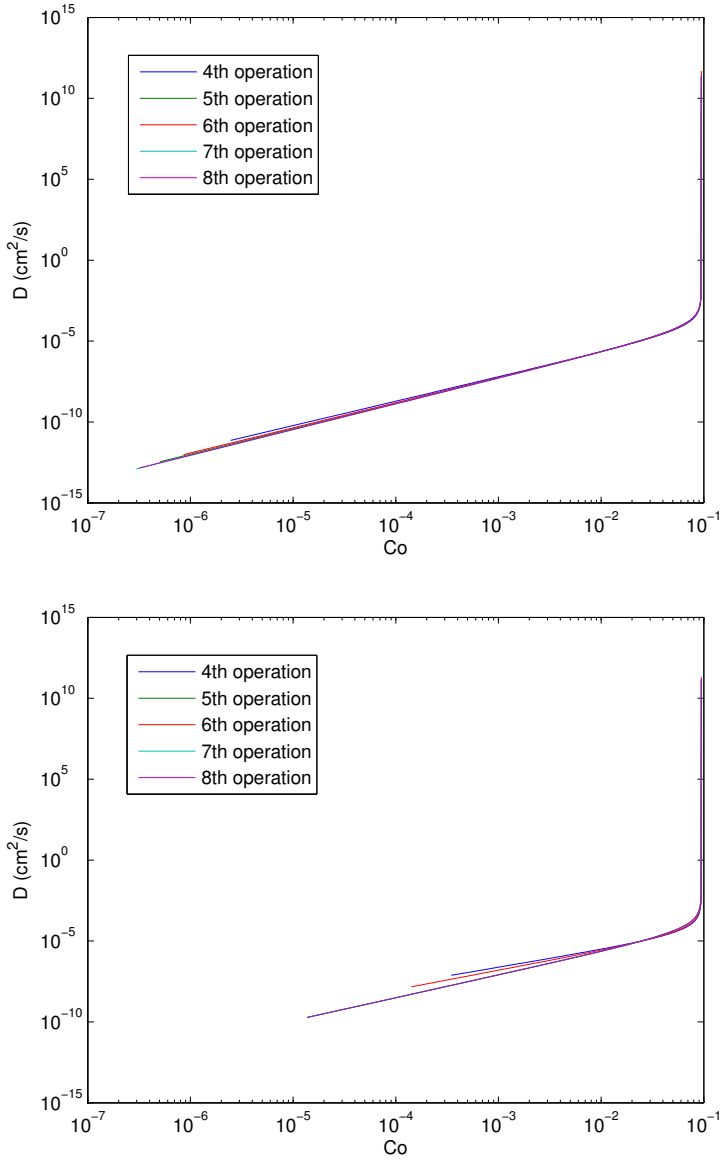

Figure 7: Impurity diffusion coefficient according to Co (a) Experiment 1 (b) Experiment 2.

3.3 Numerical simulation for the radius of the diffusion boundary

Substituting Eq. (2.10), Eq. (3.3) and Eq. (3.5) into Eq. (3.4), an ODE for R_b is derived :

$$\frac{dR_b}{dt} = 10^{-2.25} \frac{4\pi n R R_b}{V(R-R_b)g'(R_b)} \left\{ \frac{g(R_b)^{1.67}}{(3V+g(R_b))^{0.67}} \right\} \tag{3.6}$$

Eq. (3.6) is numerically integrated to predict $R_b(t)$ and the impurity concentration distributions inside the polymers at 1800 seconds is computed using Eq. (2.6) as shown in Fig. 8. C_{M0} of the 5^{th} operation is used in computing. R_b in Fig. 8. (a) decreases with time but does not reach the equilibrium state where the R_b becomes zero until 1800 seconds. R_b at 1800 seconds is illustrated in Fig. 8. (b). The impurity concentration inside the boundary has the same value as the C_{M0} and the impurity concentration outside the boundary decreases with radial distance. Since we assumed the operation time is enough for the washing process reaching the equilibrium states in previous D computing step, there exist some errors in the results. The rapid increases of D values near the end points in Fig. 6 and Fig. 7 are expected to be caused by these errors. However, these errors are expected to be negligible in computing steps deriving C_{MR} and R_b because the impurity amount inside the diffusion boundary is very small compared with the impurity amount in batch.

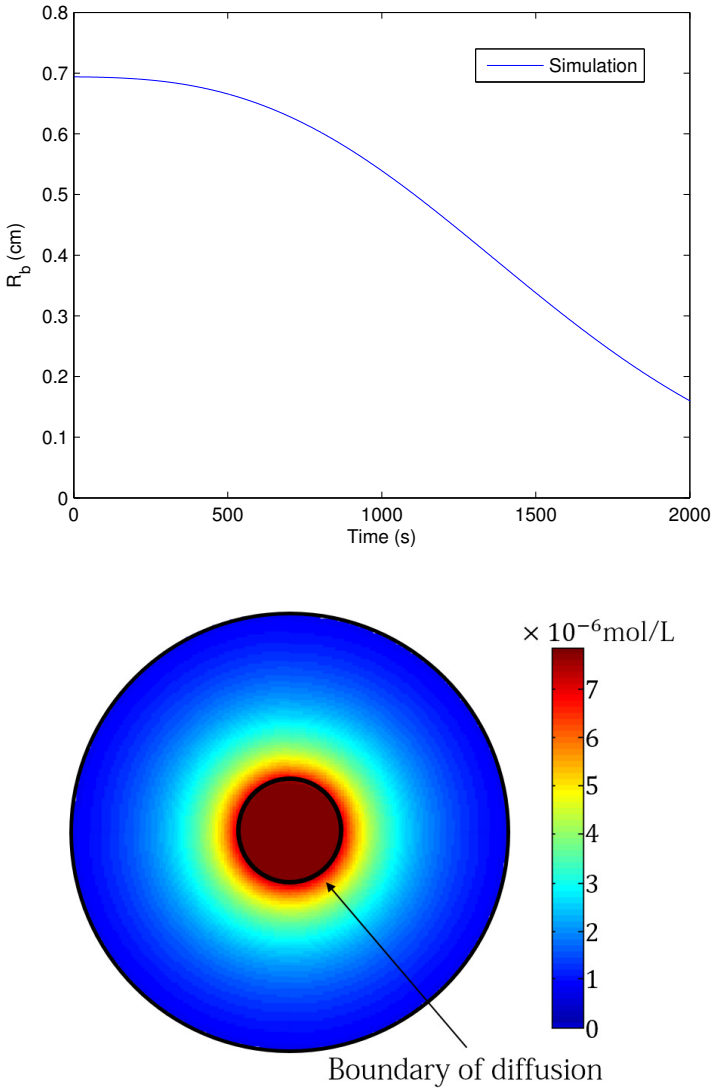

Figure 8: Simulation results of (a) radius of diffusion boundary with time (b) impurity concentration distribution inside the polymers at 1800 seconds.

Chapter 4

Model Validation

We performed validation experiments with the same SPAEK sample in a different experimental condition. 3g of polymers were washed with 50ml of 50°C deionized water 8 times for 30 minutes in each operation. The experimental condition is described in Table 3. We estimated D values of the validation experiment from the experimental condition, numerically simulated the pH changes of each operation, and validated the model by comparing the simulation results with the experimental data.

Table 3: Summary of the experimental condition in validation experiment.

Condition	Value	Unit
Average radius of polymers, R	0.75	cm
Volume of polymers, V_p	7	ml
Volume of water in batch, V	50	ml
Volume of water inside the polymers, V_{in}	4.1	ml
Volume ratio of polymer inner water to polymers, ϕ	0.59	
Number of polymer pieces, n	4	
Mass of polymers, m	3	g

4.1 Estimation of impurity diffusion coefficient at polymer surface

We divide Eq. (3.4) into two parts as

$$D = \left[\frac{V}{4\pi nR(1-Co)}\left\{\frac{3R-F(Co)}{-R+F(Co)}\right\}\right]\cdot\left[\frac{dCo}{dt}\right] = A\cdot B \qquad (4.1)$$

Part A includes the experimental condition as the coefficients, and part B is the rate of Co change which is the operational characteristic of the polymer washing process. Thus, we expect the influence of the experimental condition change on part B is negligible compared to that on part A. With this, we estimate the D values of the validation experiment by substituting the experimental condition in Table 3 and part B value of the previous experiments into Eq. (3.5)

$$D_v = 10^{-1.96}Co^{1.67} \qquad (4.2)$$

D_v is the impurity diffusion coefficient at polymer surface of the validation experiment.

4.2 Numerical simulation for pH changes and model validation

Through the same process described in Section 3.3, we simulate the R_b values of each operation using Eq. (4.2). Then, we derive the pH values of each operation using Eq. (2.10) and Eq. (3.2). Since the used SPAEK sam-

ples are identical in the previous experiments and the validation experiment, $C_{M0,1}$ is considered the same as that of the previous experiments.

The simulation results are compared with the experimental data to verify the validity of the proposed model and the experimental investigation results (see Fig. 9). We can see the simulation results of the 2-8th operations are almost in agreement with the experimental data showing low mean square errors. However there exist some discrepancies in value and shape between the simulation and experimental results of the 1st operation. This can be attributed to the same reasons explained in Section 2 that the high basicity due to the high concentration of K_2CO_3 in the 1st operation triggers the DMSO dissociation and the acidity of the DMSO affect the pH values of early operations. Consequently, the proposed model can be used to estimate D and predict the pH changes, thereby the concentration changes of the impurities, of the general polymer washing process.

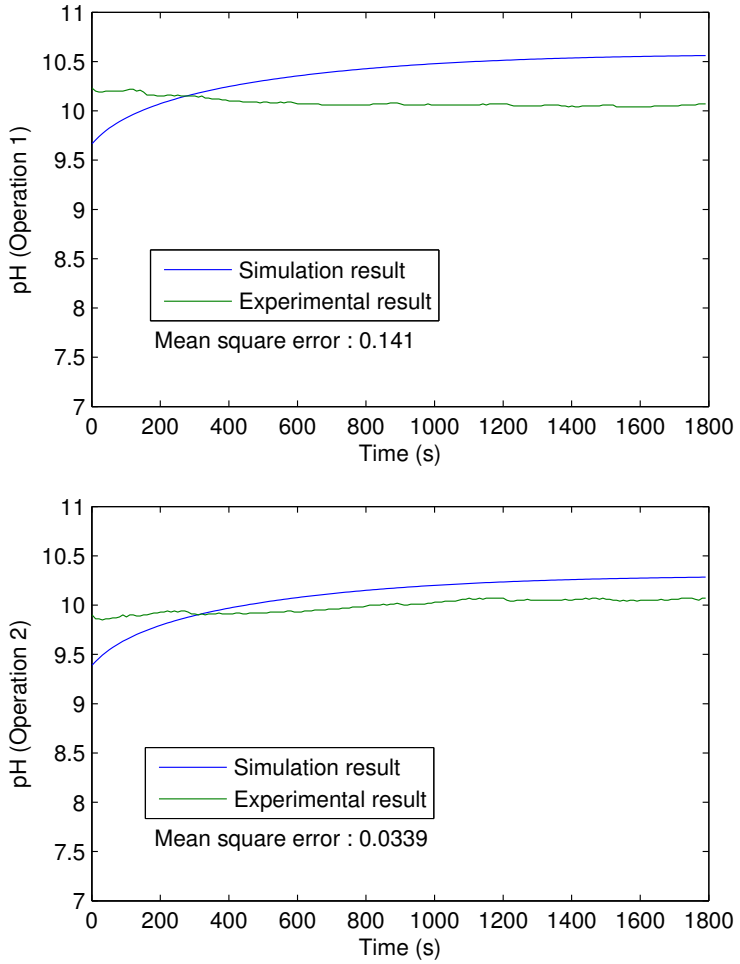

Figure 9: Comparison of the simulation results with the experimental results of the validation experiment (a) Operation 1 (b) Operation 2.

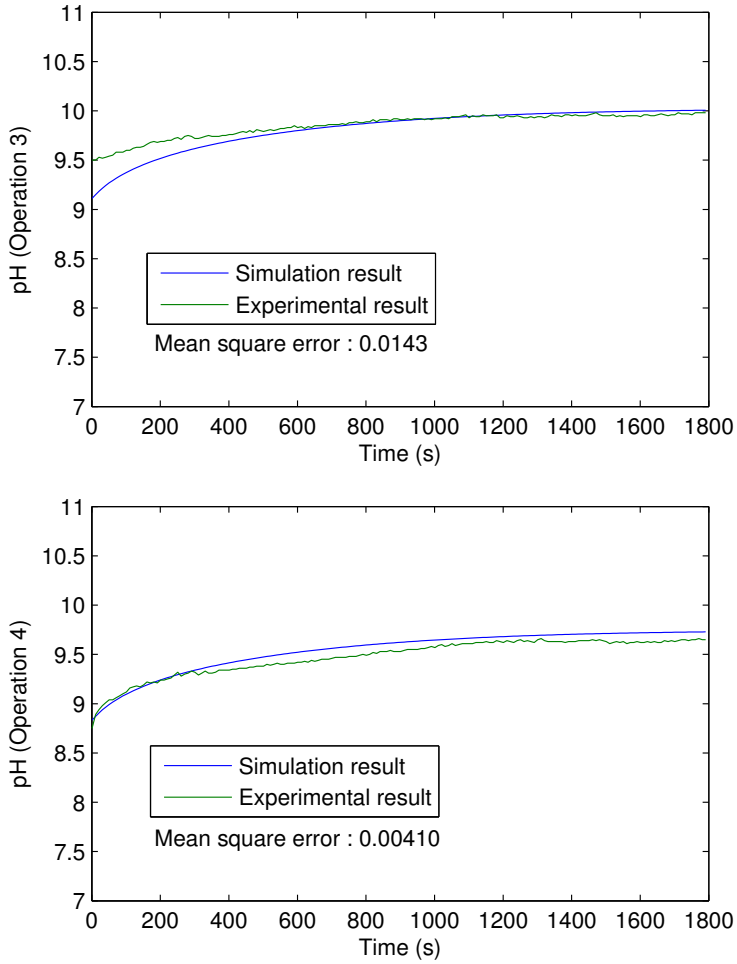

Figure 10: Comparison of the simulation results with the experimental results of the validation experiment (a) Operation 3 (b) Operation 4.

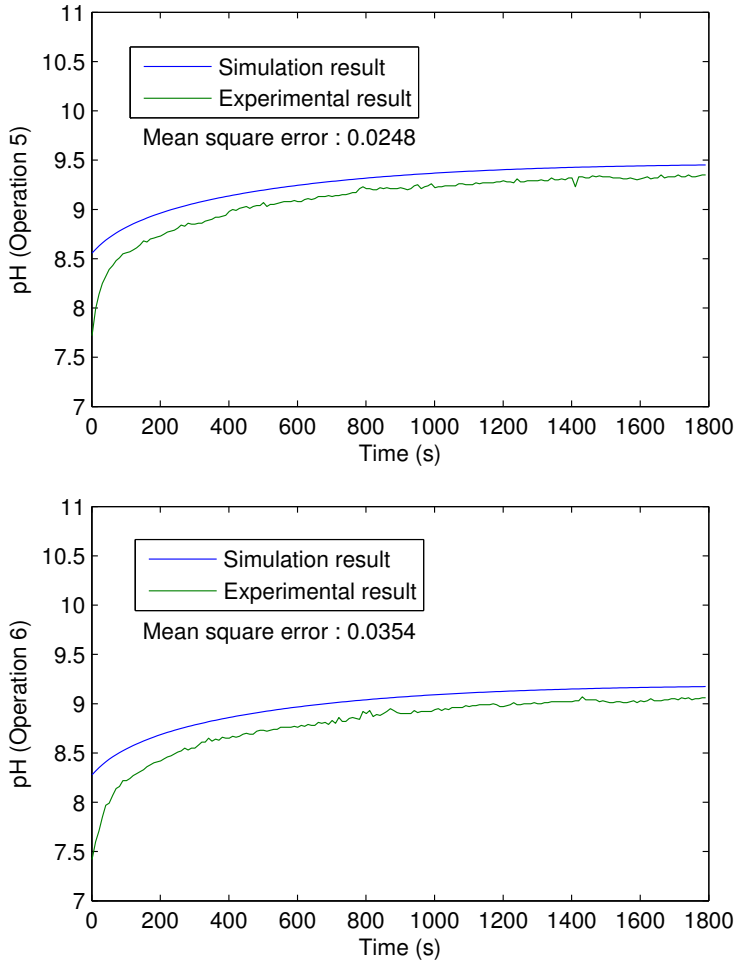

Figure 11: Comparison of the simulation results with the experimental results of the validation experiment (a) Operation 5 (b) Operation 6.

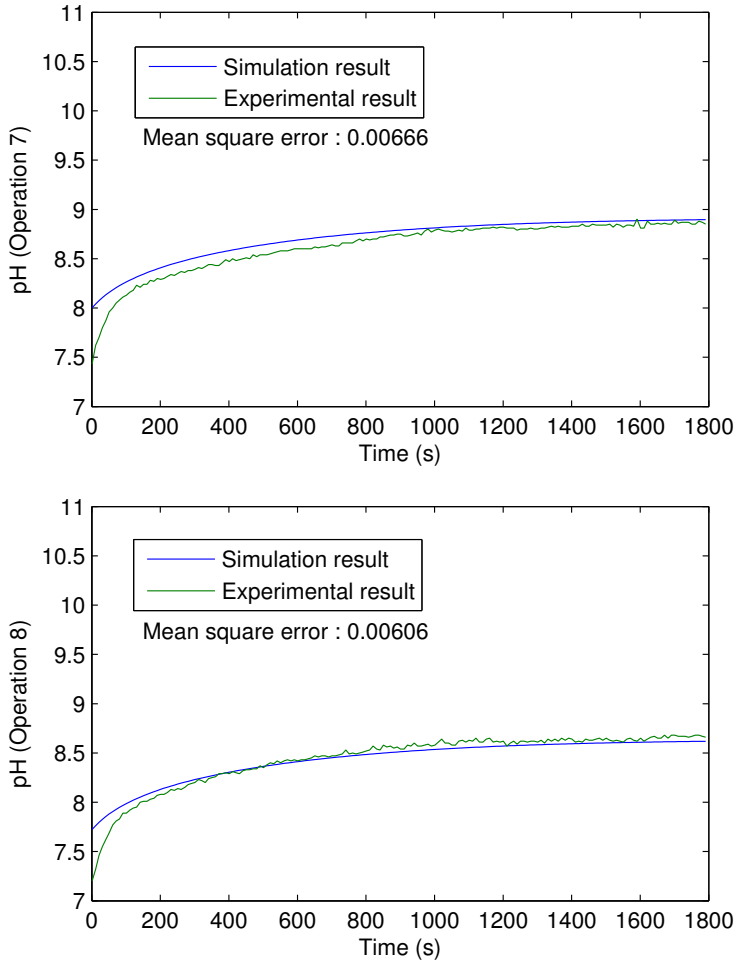

Figure 12: Comparison of the simulation results with the experimental results of the validation experiment (a) Operation 7 (b) Operation 8.

Chapter 5

Conclusion

We developed the model for the polymer washing process described by the Fick′s Law, because there exist no factors for impurity diffusion such as fluid bulk flux and electric potential gradient inside the polymers except the molecular diffusion by concentration gradient. Though the simulation results of the validation experiment are not in agreement with the experimental results of the 1st operation, they agree fairly well with the data of the 2-8th operations. This means the proposed model using the basic expectation of the impurity diffusion, the concept of moving boundary of diffusion and the pseudo steady state approximation is suitable for predicting the impurity concentrations of the polymer washing process. We can also see the D values for each operation show the same trajectory according to Co in Fig. 7. This implies other impurity diffusion factors embraced in D are only affected by Co, even if the initial impurity concentrations inside the polymers are different for each operation and the introduction of Co is proper in investigation on D.

This work has significance for providing a valid fundamental model and suitable experimental investigation procedure for polymer washing process. Using this model, the pH and impurity concentration changes of the polymer washing process which are important theoretical basis for opti-

mization and automation of polymer washing process can be predicted. In addition, the proposed model and experimental investigation methodology can be used in various kinds of polymer washing processes.

References

[1] M. Ajioka, K. Enomoto, K. Suzuki, and A. Yamaguchi, 1996. The Basic Properties of Poly(lactic Acid) Produced by the Direct Condensation Polymerization of Lactic Acid. Journal of Environmental Polymer Degradation. 3, 225-234.

[2] Yoshihiro Ohta, Shuichi Fujii, Akihiro Yokoyama, Taniyuki Furuyama, Masanobu Uchiyama, and Tsutomu Yokozawa, 2009. Synthesis of Well-Defined Hyperbranched Polyamides by Condensation Polymerization of AB2 Monomer through Changed Substituent Effects. Angew. Chem. 121, 6056-6059.

[3] Yutaka Nanashima, Akihiro Yokoyama, and Tsutomu Yokozawa, 2012. Synthesis of Well-Defined Poly(2-alkoxypyridine-3,5-diyl) via Ni-Catalyst-Transfer Condensation Polymerization. Macromolecules. 45, 2609-2613.

[4] Peixiang Xing, Gilles P. Robertson, Michael D. Guiver, Serguei D. Mikhailenko, and Serge Kaliaguine, 2004. Sulfonated Poly(aryl ether ketone)s Containing the Hexafluoroisopropylidene Diphenyl Moiety Prepared by Direct Copolymerization, as Proton Exchange Membranes for Fuel Cell Application. Macromolecules. 37, 7960-7967.

[5] Jianhua Fang, Xiaoxia Guo, Satoshi Harada, Tatsuya Watari, Kazuhiro Tanaka, Hidetoshi Kita, and Ken-ichi Okamoto, 2002. Novel Sulfonated Polyimides as Polyelectrolytes for Fuel Cell Application. 1. Synthesis, Proton Conductivity, and Water Stability of Polyimides from 4,4-Diaminodiphenyl Ether-2,2-disulfonic Acid. Macromolecules. 35, 9022-9028.

[6] Agnieszka K. Holda, Marjan De Roeck, Katrien Hendrix, Ivo F. J. Vankelecom, 2013. The influence of polymer purity and molecular

weight on the synthesis of integrally skinned polysulfone membranes. Journal of Membrane Science. 446, 113-120.

[7] B. Bittner, B. Ronneberger, R. Zange, C. Volland, J. M. Anderson and T. Kisselt, 1998. Bovine serum albumin loaded poly(1actide-co-glycolide) microspheres: the influence of polymer purity on particle character istics. Journal of Microencapsulation. 15, 495-514.

[8] Peixiang Xing, Gilles P. Robertson, Micahel D. Guiver, Serguei D. Mikhailenko, Serge Kaliaguine, 2004. Sulfonated Poly(aryl ether ketone)s Containing Naphthalene Moieties Obtained by Direct Copolymerization as Novel Polymers for Proton Exchange Membranes. Journal of Polymer Science Part A: Polymer Chemistry. 42, 2866-2876.

[9] J. Crank, 1956. Two methods for the numerical solution of moving-boundary problems in diffusion and heat flow. Q. J. Mechanics Appl Math. 10, 220-231.

[10] P. V. Danckwerts, 1950. Unsteady-state diffusoin or heat−conduction with moving boundary. Trans. Faraday Soc. 46, 701-712.

[11] Bernard P. Boudreau, 1997. Diagenetic Models and Their Implementation: Modelling Transport and Reactions in Aquatic Sediments. Springer.

[12] Dan Luss, 1968. On the Pseudo Steady State Approximation for Gas Solid Reactions. The Canadian Journal of Chemical Engineering. 46, 154-156.

[13] Murali Sankar Venkatramana, Ivan S. Colea, Bosco Emmanuelb, 2011. Model for corrosion of metals covered with thin electrolyte layers: Pseudo-steady state diffusion of oxygen. Electrochimica Acta. 56, 7171-7179.

[14] Moon-Sung Kang, Kye-Sang Yoo, Suk-Jung Oh, Seung-Hyeon Moon, 2001. A lumped parameter model to predict hydrochloric acid recovery in diffusion dialysis. Journal of Membrane Science. 188, 61-70.

[15] Denise McKay and Anna Stefanopoulou, 2004. Parameterization and Validation of a Lumped Parameter Diffusion Model for Fuel Cell Stack Membrane Humidity Estimation. Acta Metallurgica. 27, 817-828.

[16] Mauro Ferrario, Giovanni Ciccotti, Eckhard Spohr, Thierry Cartailler and Pierre Turq, 2002. Solubility of KF in water by molecular dynamics using the Kirkwood integration method. Journal of chemical physics. 117, 4947-4953.

[17] Robert C. Moore, Robert E. Mesmer, and John M. Simonson, 1997. Solubility of Potassium Carbonate in Water between 384 and 529 K Measured Using the Synthetic Method. J. Chem. Eng. Data. 42, 1078-1081.

[18] R. G. Lebel and D. A. I. Goring, 1962. Density, Viscosity, Refractive Index, and Hygroscopicity of Mixtures of Water and Dimethyl Sulfoxide. Journal of chemical and engineering. 7, 100-101.

초 록

회분식 고분자 세척공정의 기초적 모델링 및 실험적 연구

서울대학교 대학원
화학생물공학부
손 상 환

고분자 중합 반응 후에는 부반응물이나 사용된 용매, 촉매 등의 불순물 성분들이 중합된 고분자 내부에 남아있게 된다. 불순물 성분들은 고분자 내부의 미세구조에 지대한 영향을 끼치므로, 세척을 통해 이러한 불순물 성분들을 제거하고 고분자의 순도를 높여야 한다. 이 과정에서의 에너지, 세척수, 시간등의 자원의 소모를 최소화하여 고분자 세척공정을 최적화하기 위해서는 해당 공정에 대한 모델이 필수적이다. 이 연구에서는 고분자 세척 공정 최적화를 위한 이론적 기초를 정립하기 위해 해당공정에 대한 기초적인 모델링을 제시하였다. 제시한 모델은고분자 내부에서 불순물 성분의 분포를 유사정상상태 가정과 이동확산경계면 개념을 도입하여 나타내었으며, 고분자 표면에서 불순물 성분의 확산을 Fick의 법칙을 도입하여 나타내었다.

또한, 이 연구에서는 실제 SPAEK (sulfonated poly(aryl ether ketone)) 고분자 샘플 세척실험을 통한 실험적 연구를 진행하였다. 이 과

정에서 고분자 표면에서 불순물 성분의 확산계수 D를 해당샘플을 이용한 세척실험 pH 데이터로부터 계산해 내었다. 계산된 D 값은 제시된 모델에 포함되지 않은 요인들을 모두 포괄한 lumped parameter로서 각 세척배치별로 다른 값을 가졌다. 하지만 이 D값들은 무차원수 Co에 대해 나타내면 똑같은 궤적을 보였다. 이를 통해 D에 포함된 불순물 확산 요인들은 각 세척배치별 초기 고분자 내부 불순물 농도가 다름에도 불구하고 Co에 의한 특정한 경향성을 가진다는 것을 밝혀내었다.

최종적으로 앞서 수행한 실험과는 다른 조건의 검증실험을 실시하고, 위에서 제시한 모델과 실험적 연구를 통해 밝혀낸 D의 Co에 대한 경향성을 바탕으로 검증실험의 pH 값을 예측하여 실제 검증실험 데이터와 비교함으로써 제시한 모델의 예측 퍼포먼스를 검증하였다.

주요어 : 고분자 세척 공정, 이동확산 경계면, 유사정상상태 가정, Sulfonated poly(aryl ether ketone)

학번 : 2014-20583